Received 21 August 2020; revised 12 October 2020; accepted 19 October 2020. Date of publication 27 October 2020; date of current version 23 November 2020.

Digital Object Identifier 10.1109/OJCOMS.2020.3034204

Optimization and Comparison of M-PAM and Optical OFDM Modulation for Optical Wireless Communication

SHOKOUFEH MARDANIKORANI [1] (Student Member, IEEE), XIONG DENG [1,2] (Member, IEEE), AND JEAN-PAUL M. G. LINNARTZ [1,3] (Fellow, IEEE)

[1]Department of Electrical Engineering, Eindhoven University of Technology, 5600 Eindhoven, The Netherlands

[2]Academy of Advanced Optoelectronics, South China Normal University, Guangzhou 510006, China

[3]Reserach Department, Signify (Philips Lighting) Research, 5656 Eindhoven, The Netherlands

CORRESPONDING AUTHOR: S. MARDANIKORANI (e-mail: s.mardanikorani@tue.nl)

This work was supported in part by the EU H2020 Project under Grant ELIOT 825651, and in part by the National Natural Science Foundation of China under Grant 62001174.

ABSTRACT Illumination LEDs, but also infrared LEDs have limited bandwidth. To achieve high throughput, one needs to modulate the LED significantly above its 3 dB bandwidth. Orthogonal Frequency Division Multiplexing (OFDM) is a popular modulation technique to cope with the frequency selectivity of the LED channel. In this article, we challenge whether its large Peak-to-Average-Power Ratio (PAPR) and resulting large DC bias are justified. We compare systems using the same power and derive how PAM and OFDM variants reach their optimum throughput at different bandwidths and differently shaped spectral densities, thus at very different Signal to Noise Ratio (SNR) profiles but nonetheless the same transmit power.When corrected for the path loss and normalized to the noise power in the 3 dB bandwidth of the LED, we call this the Normalized Power Budget (NPB). OFDM can exploit the low-pass LED response using a waterfilling approach. This is attractive if the NPB exceeds 60 dB. OFDM will then have to spread its signal over more than ten times the LED bandwidth and requires a DC bias of more than 4 times the rms modulation depth. Second-order distortion and LED droop may then become a limitation, if not compensated. At lower power (NPB between 30 and 60 dB), DCO-OFDM outperforms PAM, provided that it significantly reduces its bias and only if it uses an appropriate adaptive bit and power loading. Without adaptive bit loading, thus using a frequency–constant modulation order, for instance made feasible by a pre-emphasis, OFDM always shows lower performance than PAM; about 2.5 dB at a NPB around 60 dB. Below 30 dB of NPB, even waterfilling cannot outweigh the need for a larger bias in OFDM, and PAM should be preferred. We argue that a mobile system that has to operate seamlessly in wide coverage and short–range high–throughput regimes, needs to adapt not only its bandwidth and its bit–loading profile, but also its DCO-OFDM modulation depth, and preferably falls back from OFDM to PAM.

INDEX TERMS LED, VLC, IR, PAM, OFDM, waterfilling, pre-emphasis, optical wireless communication.

I. INTRODUCTION

THE RAPID growth of bandwidth-intensive mobile applications combined with the emerging Internet-of-Things (IoT) services are putting immense pressure on the Radio Frequency (RF) spectrum. Recently, Optical Wireless Communication (OWC) has gained research attention from both academia and industry to provide an alternative technology for the currently predominantly RF-based connectivity [1]–[4]. OWC, employing visible light (denoted as Visible Light Communication, VLC) or the Infrared spectrum (denoted as IR communication), offers unique features, such as free access to huge amounts of unregulated but

TABLE 1. Current work in comparison with the previously published works.

		[11]	[12]	[15]	[16]	[17]	[18]	**This work**
OFDM	Clipping noise	Filtered	Flat/white	Filtered	Filtered	Filtered/white	Flat	Filtered/colored
	Mod.[1] depth optimization	Numerically	Numerically	No[3]	Numerically	Yes	N.A.	Yes
	Bandwidth optimization	Numerically	Numerically	No	Numerically	Yes/No[6]	N.A.	Analytically
	Channel model	LPF /multipath	1^{st} LPF[2]	1^{st} LPF	Cosine	Dispersive[7]/flat	flat (1 Hz)	Exponential
	Power/bit loading	Waterfilling	Waterfilling	N.A.[4]	Waterfilling	Waterfilling	N.A	Waterfilling/P.E.[10]
	Throughput expressions	No	No	No	No	No	in 1 Hz	Expressions
PAM	Constellation optimization	No	Numerically	No	No[5]	N.A.	N.A.	Analytically
	Low-pass mitigation	Equalizer	Equalizer	Equalizer	No	N.A.	N.A.	Pre-emphasis
	Bandwidth optimization	No	Numerically	No	No	N.A.	N.A.	Yes
	Power constraint	Optical	Optical	N.A.	N.A.	Opt.[8]/Elec.[9] ($V_0 = 0$).	Opt/Elec.	Versatile

[1] Modulation. [2] Low pass filter. Briefly covered in numerical simulations. [3] PAM and OFDM variants are compared for 1, 2 and 3 bit/s/Hz of data rate. [4]Not Applicable. [5] Only OOK is discussed. [6] Yes for dispersive channels and No for flat channels. [7] Time domain impulse response was used. [8] Optical. [9] Electrical. [10] Pre-emphasis.

largely interference–free bandwidth, a high degree of spatial reuse, secure connectivity, and absence of electromagnetic interference.

The output optical flux of commercial Light Emitting Diodes (LEDs), illumination or IR LEDs, is modulated in an Intensity Modulation Direct Detection (IM/DD) OWC system. This optical channel, typically, exhibits a low–pass frequency response with a 3 dB bandwidth that is dominated by LED properties which are not optimized for communication purposes. This low–pass nature, in particular the LED junction capacitance attenuates higher frequencies in the intensity-modulated spectrum [3], [5]–[8]. In this respect, line-of-sight OWC differs from Rayleigh or Rician distributions in radio communication where frequency-selective fades are sufficiently narrow to be overcome by coding and interleaving, employed in IEEE 802.11a/g standard. In OWC, excessive attenuation occurs in too wide portions of the bandwidth to rely on coding.

To handle the low-pass nature of LEDs, Orthogonal Frequency-Division Multiplexing (OFDM) yet adapted for optical applications (denoted as Optical OFDM, O-OFDM) is popular [9], [10]. There is a persistent debate on whether multi-carrier OFDM outperforms carrier–free modulation, such as Pulse Amplitude Modulation (PAM) over an OWC low-pass channel. In fact, O-OFDM allows one to optimize the distribution of the available modulation power among the sub-carriers and to select the bit load independently on every sub-carrier to maximize the data rate [5]. However, the OFDM composition of multiple frequency components has a high Peak to Average Power Ratio (PAPR) that increases the power consumption. A large DC bias needs to accommodate peaks in the signal. OFDM also requires highly linear amplifiers, which are inefficient. In an OWC link, a pre-emphasis filter can be used in front of the LED to flatten the channel frequency response. In this case, OFDM might no longer be needed. In such a flattened channel, using the simpler PAM modulation with lower PAPR reduces the biasing power waste [11], [12]. A comparison involves consideration of many aspects, which we further extend in this article.

Depending on the application, the constraint on the channel differs. For VLC, the DC power is already available for the illumination and the modern LEDs are designed to have a high wall-plug-to-lumen efficiency. However, modulation costs extra electrical power that can deteriorate the overall system efficiency and has to be limited. Thus, for VLC, *extra* consumed power is the key constraint, rather than total electrical power [13]. Particularly for IR, human eye safety can limit the average optical power to be transmitted by the LED [14].

To have a fair comparison of PAM and DC-biased Optical OFDM (DCO-OFDM) under certain constraints, one needs to operate both systems at their particular optimum. A proper framework includes for OFDM:

- optimum sub-carrier–dependent bit and power loading,
- optimized total bandwidth, and
- optimum bias current and modulation depth, in relation to the optimally tolerated clipping level, considering a realistic non-linear LED model (clipping, static and dynamic higher–order terms),

includes for PAM:

- pre-emphasis, with associated back-off to adhere to the power constraint and
- optimum bandwidth and modulation order as, in contrast to non-dispersive AWGN channels adhering to Shannon limits, we see that for the LED channel, the optimum does not necessarily lies at the smallest constellation (e.g., 2-PAM) and using the corresponding large bandwidth,

and for both modulation methods addresses

- the type of (extra) electrical or optical power constraint imposed by the application, and
- the low-pass LED response.

The comparison of different modulation schemes was studied extensively. For instance, [11], [12], [15] and [16] compare OFDM variants with a PAM scheme, while [17], [18] address OFDM variants. In fact, with respect to the above listed aspects, previous papers known to us lack at least one aspect or do not generalize their findings into generic expressions that extend outside the simulation range. We summarize the comparison between prior art and this work in Table 1.

DCO-PAM, thus level-shifted, non-negative PAM was found in [11] to outperform all variants of OFDM in terms of optical power efficiency (including DC bias power) over a range of spectral efficiencies. In [11], a Decision Feedback Equalizer (DFE) was used to combat the LED low-pass

nature and the optimization of the bit loading in OFDM could not revert this finding. However, the DFE has a high complexity, while we show that already with a simple pre-emphasis filter, PAM can become attractive, provided that also the constellation size is optimized for the LED response, in particular allowing $M = 8, ..$ for high Signal to Noise Ratio (SNR). In fact, [11] used 2 and 4-PAM only, presumably because of the DFE restrictions.

Numerical optimization for a constrained peak optical power in [12] showed that in a limited bandwidth, DCO-PAM performs better. However, in contrast to RF, the bandwidth in unregulated OWC is a design freedom that preferably is not a priori restricted. We see that for the same transmit power constraint, different modulation methods and different constellations each have a different optimum bandwidth, and that it leads to different SNR profiles along the frequency axis. Hence SNR is not a preferred benchmark.

In DCO-OFDM, the modulation depth, relative to the DC-bias determines the amount of clipping. This may prohibit the use of larger modulation orders. In [12], clipping noise was assumed to have a flat spectrum at the receiver over all FFT outputs regardless of the actual signal bandwidth. However, we show that the clipping noise predominantly depends on the modulation bandwidth. That is, one cannot arbitrarily spread clipping noise outside the signal bandwidth by using faster, oversized FFT processing at the receiver. Moreover, the clipping artefacts further are subject to the low–pass LED frequency response. As shown in Table 1, this was simplified in previous works.

The work in [15] compares single–carrier (but frequency–domain equalized) M-PAM modulation to multiple OFDM variants, with a main focus on multi-path dispersion of the OWC propagation channel. M-PAM appeared to require a lower SNR to achieve the same Bit Error Rate (BER). Both LED clipping and low-pass memory effects are covered in numerical simulations. However, no further optimizations for modulation bandwidth nor for a (frequency–adaptive) modulation order are discussed. On-Off Keying (OOK) shows a better optical power efficiency than DCO-OFDM and unipolar Asymmetric Clipped Optical OFDM (ACO-OFDM) in single-mode fiber systems [16], where the DC bias and bandwidth optimizations were carried out by numerical simulations, considering clipping for low biases. In fact, at low available transmit power, ACO-OFDM can become more attractive than DCO-OFDM [11], [19]. However, Section VII-B2 shows that PAM reaches higher throughput for the same power.

In [17], OFDM has been studied for VLC in flat and dispersive channels, addressing also clipping noise while optimizing the DC offset of OFDM. However, the practical limitations of a discrete modulation order and an optimization of the modulation bandwidth for OFDM were not discussed. On a pre-emphasized channel, the use of a fixed number of constellation bits over a fixed (non-optimized) bandwidth causes pronounced, abrupt discontinuities in the throughput, versus changes in the SNR [5]. That is, e.g., if the receiver gradually moves away from the transmitter, there will be a stepwise, non-graceful cut-off in throughput. In [18], throughput achieved by OFDM-based schemes were discussed. The clipping noise as well as the distortion introduced by the LED are modelled. However, the results of [18] did not include the frequency selectivity of the LED channel.

To optimize OFDM for frequency selective LED channels, different power and bit loading strategies have been discussed in the literature, e.g., [5], [20]–[25]. Waterfilling and uniform bit loading (also known as pre-emphasized power loading) are the two well-known strategies. Waterfilling is known as the optimum strategy that results in the maximum throughput in a frequency selective communication channel [20]. However, it requires a (relatively) complex algorithm [5], [21], [22]. The existing ITU g.9991 standard [26] simplifies this into assigning the same power level to all sub-carriers, but adapts the constellation per sub-carrier. Forcing a uniform constellation on all sub-carriers would further simplify the implementation to a great extent [25]. This is also considered in the current standardization of IEEE 802.11bb [27], as it can reuse approaches designed earlier for RF channels. In this work both waterfilling and pre-emphasis strategies are considered.

The main contributions of this work include the following:

- In many other communication channels, using a higher bandwidth enhances throughput. In contrast to this, we show that for an LED there exists an optimum modulation bandwidth beyond which the throughput reduces. Moreover, OWC standards that fix bandwidth, as radio standards typically do, abruptly fail to sustain a weakening link.
- To make a fair comparison among systems that optimize their transmit bandwidth, we introduce the Normalized Power Budget (NPB), defined as transmit power corrected for path loss, normalized to the noise in the 3 dB bandwidth of the LED. In fact, we cannot use the bandwidth of transmit signal as different modulation strategies optimize differently.
- We derive mathematical expressions for the throughput and the preferred modulation bandwidth for DCO-PAM and DCO-OFDM. Using the now commonly reported exponential OWC channel frequency response [28], [29], we capture these in new expressions. Hitherto, the comparisons were mostly limited to simulations for specific settings, thereby did not give generic expressions for other settings. Furthermore, we derive expressions for the optimum modulation bandwidth for DCO-OFDM and for (DCO-) PAM, considering discrete modulation orders and optimizing for the LED low-pass response. Our optimization includes the impact of limiting the DC bias for an OFDM signal, by allowing clipping and by making a trade off with the resulting clipping noise.

- We quantify clipping for DCO-OFDM as it raises the perceived noise floor and thereby limits the usable modulation order, even in a further noise–free channel. Following arguments in [5], [11], [17], [30], [31], we conclude that for modern LEDs, a saturation peak limit does not accurately model the behavior. We use and extend the clipping noise model of [17] which considered one-sided clipping of the LED current. This extends our previous bit loading evaluations in [5], which assumed clipping-free DCO-OFDM, leading to more complete, realistic model.
- We compare constrained optical power (related to the average LED current), the extra electrical power (related to the variance of the current caused by modulation) and the total electrical power (related to a combination of DC current and AC variance, weighted by the LED (say, bandgap) voltage and the dynamic resistance, respectively). While previously published works, e.g., [11], [12], [15], and [16], often report outspoken preferences for the choice of modulation, we conclude that there is not always simple unique answer to the question whether OFDM and PAM is performing better, depending on which constraint applies.
- We show that in a VLC context, where the extra power needs to be far below the illumination power, there is no difference in performance between pre-emphasized DCO-OFDM and a DCO-PAM. However, DCO-OFDM with waterfilling outperforms DCO-PAM.
- For IR, where the bias or the mean DC light has to be paid for from the communication power budget, PAM with an appropriate high-boost and a carefully chosen bit rate and bandwidth outperforms pre-emphasized OFDM. Our model of the impact of clipping artefacts allows us to optimize the choice of the modulation depth for OFDM. In fact, one can intuitively interpret our results as a quantification that the power penalty incurred for the DC bias in pre-emphasized DCO-OFDM is not compensated by the ability to adaptively load sub-carriers over a certain NPB range. For high power budgets, say NPB above 30 dB, however, OFDM with waterfilling and optimum choice of LED bias current outperforms PAM. Here, OFDM can fully exploit the adaptive bit and power loading. For high power budgets one can afford a large back-off of the modulation depth to avoid clipping of the OFDM signal, the latter conclusion disagrees with [12]. We show that the crossover point where OFDM with waterfilling outperforms PAM moves to higher power budget values when LED is biased at higher currents. If, instead, more LEDs were used to boost coverage, this would not happen.
- We propose a simple rule of thumb and an algorithm to optimize the modulation order and the modulation bandwidth of M-PAM, which works for both VLC and IR applications.

The rest of the paper is organized as follows. We start with a short introduction to the OWC link and the realistic LED channel model in Section II. Section III presents the DCO-PAM model, its performance over an OWC channel and the DC penalty required. DCO-OFDM is discussed in Section IV. Both the continuous (for theoretical purposes) and discrete (practical case) modulation orders are discussed. This section also presents the optimum waterfilling approach results for the comparison. The DC penalty and the clipping noise associated with DCO-OFDM is discussed in Section V. In Section VI a proper measure is given to choose a proper DC bias for the LED based on the modulation order. Furthermore, this section includes the distortion power due to clipping (to reduce the DC penalty) of the LED current in the throughput and modulation bandwidth requirement. Section VII compares DCO-OFDM and DCO-PAM in three different contexts, VLC, IR and average–optical–power constrained channels. The computational complexity of DCO-OFDM and PAM is discussed in Section VIII. Finally, conclusions are drawn in Section IX.

II. OWC POWER CONSTRAINTS

Various LED models are used in scientific literature. This section elaborates on our LED model, that considers non-negativity, junction voltage and LED junction capacitance and resistances. So, in fact following [5], we consider LED low–pass nature and one–sided clipping. We model that electrical power consumption not only grows with the DC bias, but also with the modulation variance. In contrast to this, the average optical power only relates to the biasing, while modulation comes for free, in the sense that DC-free modulation does not affect the average current. We denote the LED current to consist of $I_{LED}(t) = \mathrm{I}_{LED} + i_{led}(t)$, where $i_{led}(t)$ is the zero–mean (AC) modulation current and I_{LED} is the DC current of the LED to ensure $I_{LED}(t) \geq 0$. The DC power consumption of the LED is, $\mathrm{P}_{DC} = \mathrm{V}_{LED}\mathrm{I}_{LED}$. Here, the DC voltage V_{LED} can be expressed as

$$\mathrm{V}_{LED} \approx \mathrm{V}_0 + R_{LED}\mathrm{I}_{LED}, \tag{1}$$

where V_0 can be interpreted as the turn-on limit and R_{LED} is the dynamic plus parasitic resistance of the LED [32], [33]. So the total electrical power consumed by the LED is,

$$\mathrm{P}_{tot} = \mathrm{V}_0\mathrm{I}_{LED} + R_{LED}\mathrm{I}_{LED}^2 + \frac{1}{\eta}R_{LED}\sigma_{mod}^2, \tag{2}$$

where σ_{mod}^2 is the variance of LED AC current $i_{led}(t)$ and where η is the modulation LED power amplifier efficiency, used in a Bias-T setting [34]. An extensive study [34] into the power efficiency of a series transistor modulator revealed a total power consumption of $P_{tot} \approx (\mathrm{V}_0 + 2R_{LED}\mathrm{I}_{LED})\mathrm{I}_{LED}$ where factor 2 is due to an extra voltage headroom $R_{LED}\{\max I_{LED}(t)\}$ required to operate the modulating series transistor [34]. More generically, a versatile power constraint is the weighted sum of moments of the probability of the signal

$$\mathrm{P}_{tot} = \mathrm{P}_{DC} + \mathrm{P}_{ext} = \beta_1\mathrm{I}_{LED} + \beta_2\sigma_{mod}^2 + \beta_3\mathrm{I}_{LED}^2, \tag{3}$$

where P_{ext} is the extra power on top of the DC power consumed by the LED due to modulation and the β-weights may also depend on the electronic topology and the use case (VLC vs IR). In fact, various papers take different interpretations of β_1, β_2 and β_3, as we will discuss in the next sections.

A. POWER CONSTRAINT

For IR and VLC communication, the power can be constrained either in the optical or the electrical domain, which may lead to different optimizations.

1) OPTICAL POWER CONSTRAINT

Optimizations for the optical domain, for instance dictated by eye-safety in IR or illumination level in VLC, basically limit the average (or DC-bias) LED current I_{LED} : ($\beta_1 > 0$, $\beta_3 = 0$), but do not impose a power penalty for modulation ($\beta_2 = 0$). As we will quantify in Section V, the DC current I_{LED} needs to accommodate the LED input current AC excursions. Hence, it nonetheless becomes an indirect function of σ^2_{mod} to ensure a sufficiently low clipping distortion.

2) ELECTRICAL POWER CONSTRAINT IN IR

The associated electrical power also depends on the variance via $\beta_2 = R_{LED}$. For a constrained total electrical power, in (2), $\beta_1 = V_0$, $\beta_2 = \beta_3 = R_{LED}$. In fact, the non-linear current-voltage curve, approximated in (1), was further simplified by omitting the photonic junction voltage ($V_0 = 0$) in [17], taking $P_{tot} = R_{LED}(I^2_{LED} + \sigma^2_{mod})$, thus $\beta_2 = \beta_3$ and $\beta_1 = 0$. Yet, V_0 dominates the voltage across the LED ($V_0 > R_{LED}I_{LED}$). Hence, OWC sees a large β_1, so that $P_{tot} \approx V_0 I_{LED}$ may be reasonable as a first-order estimate, particularly if V_0 is adjusted for typical biased V_{LED} voltages.

3) EXTRA POWER CONSTRAINT IN VLC

The primary function of VLC is illumination, so the DC current of the LED is determined by the target illumination level [18], and is not subject to a communication optimization ($\beta_1 = 0, \beta_3 = 0$). As communication is a secondary function, the illumination system is expected to deliver a high lumen-per-wall-socket-watt. Consequently, any additional consumption of power just for modulation deteriorates the energy efficiency and may even jeopardize the 'green' certification of the LED lighting product. Hence, an important VLC design objective is to get the highest possible throughput for the least amount of extra power, in a regime where DC bias is not the dominant scarce resource. In fact, modulating the LED current consumes extra power $P_{ext} \approx R_{LED}\sigma^2_{mod}/\eta$, as reflected in $\beta_2 = R_{LED}/\eta$ [5], [19]. An (in-) efficiency of the amplifier (LED driver) can be reflected in η. If we are only interested in the LED power, we take $\eta = 1$. However, inefficient (linear) modulator amplifiers in VLC make the overall LED lighting product less efficient, even to the extend that it fails lighting energy conservation regulations [5]. Hence, VLC optimizations on P_{ext} are highly relevant (thus with $\beta_1, \beta_3 = 0$). In this article, we evaluate systems limited by extra power in Section VII-A.

B. CHANNEL MODEL

The low-pass frequency response of the LED channel from LED current to photodiode current can be modeled as a low-pass filter [5], [28], [29],

$$|H(f)|^2 = H_0^2 2^{-f/f_0}, \tag{4}$$

where H_0 and f_0 are the low frequency channel gain and the 3 dB cut-off frequency, respectively.

We focus on Line-of-Sight (LoS) channels. In fact, we increasingly see the creation of beam steering emitters and of angular diversity receivers. In such case, each resolved angular path is not likely to be subject to a significant delay spread. Hence, we believe that the reflection-free LoS assumption remains relevant. If nonetheless long delay spreads occur, a linear time–domain equalizer can become complex for PAM, and frequency–domain equalization may be preferred, as in OFDM [15].

C. NORMALIZED POWER BUDGET (NPB) DEFINITION

Often, systems are compared based on the (frequency–average) SNR at the receiver, for a particular choice of the modulation bandwidth. However, this leads to an intrinsically unfair comparison as PAM and OFDM benefit differently from expanding the modulation bandwidth further beyond the LED 3 dB bandwidth. In fact, bandwidth is a parameter subject to modulation–specific optimization constrained by transmit power (see for instance Figure. 1 and Figure. 4). This prohibits us to compare two systems just with the same bandwidth or with the same SNR. Although, it seemingly complicates the number of variables, we must restrict a comparison to essential parameters that are not a design freedom. We use H_0, f_0, the modulation rms σ^2_{mod} and the noise spectral density N_0, represented in A^2/Hz, referenced to currents through the photodiode detector at the receiver and we define the NPB γ as

$$\gamma = \frac{\sigma^2_{mod} H_0^2}{N_0 f_0}. \tag{5}$$

In fact, normalizing to the LED bandwidth f_0 and not to signal bandwidth f_{max} allows us to plot generic curves for throughput. To optimally cope with the frequency-dependent channel response $H(f)$, we take the freedom to optimize the emitted spectral density $S_x(f)$ and the total bandwidth. The subscript x indicates the modulation strategy; PAM for DCO-PAM, p for DCO-OFDM with pre-emphasis and w for DCO-OFDM with waterfilling. The noise bandwidth is subject to dynamic adaptations and the SNR is frequency dependent:

$$\mathrm{SNR}(f) = \frac{S_x(f)|H(f)|^2}{N_0}. \tag{6}$$

We denote the frequency-domain spectral density of $i_{led}(t)$ by $S_x(f)$, expressed in A^2/Hz. Over the signal bandwidth, $S_x(f)$ integrates to σ^2_{mod}. That is,

$$\int_f S_x(f) df = \sigma^2_{mod}. \tag{7}$$

Here, σ^2_{mod} and γ address effective signal powers thus allow the calculation of link performance, but ignore DC-biasing power. We relate these to consumed power later when we invoke β weight factors.

For a pre-emphasized spectrum, the received modulation spectrum after the photodiode, $S_x(f)|H(f)|^2$, is flat over frequency. To achieve this, $S_x(f)$ inverts $H(f)$ according to

$$S_x(f) = \kappa \frac{\sigma^2_{mod}}{f_x} 2^{f/f_0}, \tag{8}$$

where κ is the pre-emphasis back-off to satisfy the constraint (7) and f_x is the modulation bandwidth over which the $S_x(f)$ is spread. Inserting (8) into (7), the coefficient κ is calculated as

$$\kappa = \frac{\ln(2) f_x/f_0}{2^{f_x/f_0} - 1}. \tag{9}$$

If, for PAM, instead of a pre-filter, a linear post-equalizer is used, the transmit current density is uniform, or fully determined by the pulse shaping. However, the receive filter will then boost the noise in every sample by κ. That is, the SNR for every PAM sample is the same for either a pre or post equalization (κ applies).

III. PULSE AMPLITUDE MODULATION (PAM)

PAM requires a flat frequency response for Inter–Symbol Interference (ISI) free communication. To repair the low–pass LED frequency response, as in (4), a linear equalizer can be used to boost high frequency components [35], [36]. According to Nyquist theory, a baseband PAM signal with a bandwidth f_{PAM} can accommodate $2Tf_{\text{PAM}}$ symbol dimensions in a time interval T. For a symbol duration T_s ($T_s = 1/(2f_{\text{PAM}})$), we multiply the numerator of the SNR in (6) by $2T_s f_{\text{PAM}}$, thus by unity, to get

$$\text{SNR}_{\text{PAM}}(f) = \frac{2S_{\text{PAM}}(f)|H(f)|^2 f_{\text{PAM}} T_s}{N_0} = \frac{2\epsilon_N}{N_0}. \tag{10}$$

where ϵ_N is the average received symbol energy per dimension. For PAM, the energy per symbol ϵ_s equals ϵ_N, while for two-dimensional QAM, as used in OFDM, $\epsilon_s = 2\epsilon_N$.

In (bi-polar) M-PAM, input data are mapped into a zero-mean sequence of symbols chosen from M discrete levels, uniformly spaced by distance $2d_M$, so

$$s_m = m d_M, \quad m \in \{\pm(M-1), \pm(M-3), \ldots, \pm 1\}. \tag{11}$$

The average energy per symbol (at the receiver), ϵ_s, is

$$\epsilon_s = \epsilon_N = \frac{2d_M^2}{M} \sum_{m=1}^{M/2} m^2 = \frac{M^2-1}{3} d_M^2. \tag{12}$$

The distance d_M can then be expressed as a function of ϵ_N as follows:

$$d_M = \sqrt{\frac{3\epsilon_N}{M^2-1}}. \tag{13}$$

TABLE 2. Required received average energy per dimension normalized to N_0 for different constellation size (M) and the minimum normalized bias requirement z at BER = 10^{-4}.

M	QAM order	$X(M)$	$X(M)$ in dB	z (OFDM)
2	4	6.92	8.4	1.11
4	16	33.23	15.2	1.69
8	64	134.61	21.3	2.15
16	256	527.49	27.2	2.57
32	1024	2055.6	33.1	2.95

The BER is expressed as [37]

$$\text{BER}_{\text{M}} = \frac{2}{\log_2 M}\left(\frac{M-1}{M}\right) Q\left(\sqrt{\frac{6\epsilon_N}{(M^2-1)N_0}}\right). \tag{14}$$

Thus, the average energy requirement of a M-PAM scheme, normalized to N_0 and denoted as $X(M)$ for a pre-determined BER_{M} is

$$X(M) = \frac{M^2-1}{6}\left(Q^{-1}\left(\frac{M\log_2 M}{2(M-1)}\text{BER}_{\text{M}}\right)\right)^2. \tag{15}$$

We list $X(M)$ in Table 2 and extend it to M^2-QAM by interpreting QAM as just a 2D variant of M-PAM. We explicitly use a different symbol $X(M)$ to represent a fixed system property, while ϵ_N/N_0 is a property of the incoming signal, subject to optimization and may even be frequency dependent.

Within a Nyquist bandwidth of f_{PAM}, a system reaches a throughput R_{PAM} of

$$R_{\text{PAM}} = 2f_{\text{PAM}}\log_2 M. \tag{16}$$

A. PAM BIAS PENALTY

For PAM as in (11), a DC-bias of at least $(M-1)d_M$ is needed to make the LED signal non-negative. We define a parameter z to be the ratio of the bias current over the LED rms current. For PAM,

$$z = \frac{\text{I}_{\text{LED}}}{\sigma_{mod}} = \frac{(M-1)d_M}{\sqrt{\frac{M^2-1}{3}}d_M} = \sqrt{3\frac{M-1}{M+1}}, \tag{17}$$

where the variance of the modulation σ_{mod} can be calculated from (11), as $\sigma_{mod} = d_M\sqrt{(M^2-1)/3}$. For such DCO-PAM, the parameter z depends on the modulation order M. It equals $z = 1$ for $M = 2$ and approaches $z = \sqrt{3}$ for $M \to \infty$. We will use this parameter in the later sections to compare PAM with OFDM.

B. THROUGHPUT OF DCO-PAM OVER LOW-PASS CHANNEL

Inserting (8) into (6) with κ given in (9) and the channel model (4), the $\text{SNR}(f)$ for PAM becomes

$$\text{SNR}_{\text{PAM}}(f) = \frac{\sigma^2_{mod}H_0^2}{N_0 f_0} \cdot \frac{\ln(2)}{2^{f_{\text{PAM}}/f_0} - 1}. \tag{18}$$

To benchmark our results, we also relate it to the NPB defined in (5),

$$\text{SNR}_{\text{PAM}}(f) = \gamma \frac{\ln(2)}{2^{f_{\text{PAM}}/f_0} - 1}. \tag{19}$$

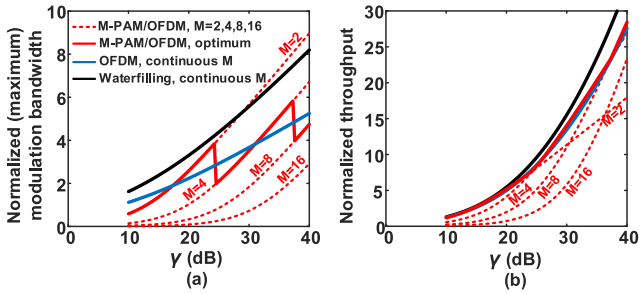

FIGURE 1. (a) (Optimum) normalized modulation bandwidth ($f_{\max_{PAM}}/f_0$, $f_{\max_P}/f_0$ and $f_{\max_W}/f_0$ for PAM, pre-emphasized OFDM and waterfilling, respectively) and (b) normalized throughput versus NPB used for modulation, γ, ignoring DC-bias power (VLC scenario). Dashed-red lines represent the performance for various constellation sizes M (for PAM and pre-emphasized DCO-OFDM) with the solid red being the choice of M optimized for maximum throughput. Solid blue and black lines represent the performance of OFDM with pre-emphasis and waterfilling, respectively, for continuous modulation order. For all plots $\text{BER}_\text{M} = 10^{-4}$.

In (10), we derived an equivalent expression for the SNR as a function of ϵ_N. From (10) and (19), the achieved ϵ_N/N_0, expressed in terms of the NPB and the bandwidth in PAM modulation is

$$\frac{\epsilon_N}{N_0} = \gamma \frac{\ln 2}{2\left(2^{f_{\text{PAM}}/f_0} - 1\right)}. \tag{20}$$

In order to support a constellation M, the ϵ_N/N_0 must exceed $X(M)$ (given in Table 2 and defined in (15)). So, we require

$$\gamma \geq \frac{2X(M)}{\ln 2}\left\{2^{f_{\text{PAM}}/f_0} - 1\right\}. \tag{21}$$

This allows us, for any NPB γ and M, to find the modulation bandwidth,

$$f_{\text{PAM}} \leq f_0 \log_2\left\{\frac{\ln 2}{2}\frac{\gamma}{X(M)} + 1\right\}. \tag{22}$$

For any M, we fully utilize the available power when f_{PAM} is set to reach an equality. For $\text{BER}_\text{M} = 10^{-4}$ and $M = 2, \ldots, 32$, we use the $X(M)$ values of Table 2 to plot f_{PAM} as a function of γ_{PAM} in Figure. 1(a), shown with dashed red lines. We use (16) to plot the throughput in Figure. 1(b) for various M as the function of γ. Normalization to f_0 allows us to plot generic curves, not specific for the bandwidth of the chosen LED.

For each γ value, the optimum value of M is the one that gives the highest throughput, shown in Figure. 1(b) with a solid red line. The corresponding optimum (or maximum) normalized modulation bandwidth $f_{\max_{\text{PAM}}}$ to achieve the maximum throughput is also shown in Figure. 1(a) with a solid red line. We learn from Figure. 1, that for a NPB (γ) up to 24.3 dB and for $\text{BER}_\text{M} = 10^{-4}$, the optimum modulation is OOK (2-PAM). In fact for a NPB below 24.3 dB, it is preferred to use a crude modulation method very far beyond the 3 dB bandwidth of the LED rather than to choose a higher constellation to stay within the LED bandwidth. This NPB also corresponds to a $f_{\max_{\text{PAM}}} = 3.85\ f_0$. This insight can be the basis for a practical algorithm to find, adapt and track the best compromise between bandwidth and M: initially search for the highest throughput that is possible with 2-PAM, by increasing the bit rate while adhering to the transmit power constant. If it turns out that for this throughput, the corresponding $f_{\max_{\text{PAM}}}$ exceeds 3.85 f_0, then the algorithm adopts 4-PAM, and searches for the new highest sustainable bit rate by scaling down f_{max}. The limits of $f_{\max_{\text{PAM}}}$ for which 8-PAM and 16-PAM are appropriate appear to be 5.8 f_0 and 7.7 f_0, respectively. For a total–power limited channel, similar numbers apply. When a communication link is operational, one preferably uses receiver feedback to change the symbol rate while keeping M fixed, but only switch up or down M at specific threshold symbol rates. Figure. 1(b) shows that the penalty for sticking to suboptimal M can be substantial. At higher NPB, sticking to 2-PAM or 4-PAM is not attractive. Similarly, sticking to a pre-configured, possibly sub-optimum $f_{\max}$, thus only adapting M, can have a significant penalty and leads to a full collapse of the link at some low γ.

IV. OFDM

OFDM can naturally handle the frequency selective LED behavior by dividing the input information over multiple sub-carriers, with a aggregate bandwidth that can be multiple times the channel 3-dB bandwidth. As each sub-carrier only occupies a small fraction of the modulation bandwidth, it sees a (relatively) flat channel frequency response. A sub-carrier at frequency f with a bandwidth Δf can accommodate $T\Delta f$ two dimensional M^2-QAM symbols in a time duration T. The duration of one OFDM block is $T_s = 1/\Delta f$. As the symbol energy equals $\epsilon_s(f) = S_x(f)|H(f)|^2 \Delta f T_s = S_x(f)|H(f)|^2$, we can rewrite the SNR as

$$\text{SNR}_{\text{OFDM}}(f) = \frac{\epsilon_s(f)}{N_0} = \frac{2\epsilon_N(f)}{N_0}. \tag{23}$$

For OFDM, each sub-carrier symbol is received with a different energy, thus preferably it is loaded with its optimized constellation $M(f)$. Therefore, we explicitly write $\epsilon_N(f)$ as a function of frequency.

A. THROUGHPUT OF DCO-OFDM OVER LOW-PASS CHANNEL

We use BER formula (14) for (two-dimensional) M^2-QAM by including the frequency dependency of $\epsilon_N(f)$. Taking the inverse of (14), the modulation order $M(f)$ of the sub-carrier at frequency f can be expressed as

$$M(f) = \sqrt{\frac{2\epsilon_N(f)}{\Gamma N_0} + 1}, \tag{24}$$

where

$$\Gamma = 1/3\left(Q^{-1}\left(\frac{M(f)\log_2 M(f)}{2(M(f)-1)}\text{BER}_\text{M}\right)\right)^2 \tag{25}$$

is the modulation gap. The gap is a slightly decreasing function of the modulation order M [5]. For simplicity we use the worst case of modulation order $M = 2$ which gives a maximum Γ for the given BER_M. This simplifies (25) into

$$\Gamma = 1/3\left(Q^{-1}\left(\frac{\text{BER}}{2}\right)\right)^2, \tag{26}$$

where BER is the total bit error rate, BER $\approx 2\text{BER}_\text{M}$. The number of bits $b(f)$ per dimension that can be delivered is

$$b(f) = \log_2(M(f)) = \frac{1}{2}\log_2\left[1 + \frac{2\epsilon_N(f)}{\Gamma N_0}\right]. \quad (27)$$

Inserting (23) and (6) results in

$$b(f) = \frac{1}{2}\log_2\left(1 + \frac{1}{\Gamma}\frac{S_x(f)|H(f)|^2}{N_0}\right). \quad (28)$$

The throughput[1] over a modulation bandwidth $[0, f_x]$ is obtained by integrating all the rate contributions, given by (28),

$$\begin{aligned} R &= \int_0^{f_x} 2b(f)df \\ &= \int_0^{f_x} \log_2\left(1 + \frac{1}{\Gamma}\frac{S_x(f)|H(f)|^2}{N_0}\right)df. \end{aligned} \quad (29)$$

The factor 2 reflects the two dimensions per second per Hz of QAM. This expression looks like a misused Shannon limit for AWGN channels, which repeatedly was argued not to be valid for optical channels. However, here (28) and (29) come just as a consequence of inverting the BER expression.

B. OFDM WITH WATERFILLING

In practice, the constellation size M can only take values from the discrete set $\{2, 4, 8, \ldots\}$. However, for theoretical derivations it is convenient to assume that M can take any arbitrary positive value, including a non-integer one. As argued in [5], regardless of the choice of $\beta_{1,2,3}$, any optimized power spectral loading is equivalent to applying constraint (7) to choose the transmitted $S_x(f)$ to maximize the throughput (29). Lagrangian optimization leads to the well-known waterfilling solution with $S_x(f)$ adhering to [20]

$$S_w(f) = \Gamma\left(\frac{N_0}{|H(f_{\max_w})|^2} - \frac{N_0}{|H(f)|^2}\right)^+, \quad (30)$$

where the subscript w refers to waterfilling and $f_{\max_w}$ is the maximum modulation frequency for which $S_w(f)$ is non-zero. The optimal power allocation of (30) shows that low frequency sub-carriers that experience a good channel quality are assigned more power than those at higher frequencies. Substituting (30) into (7) and solving the integral relates the optimum modulation $f_{\max_w}$ to the NPB γ:

$$\gamma = \frac{\Gamma}{\ln(2)}\left(1 + \left(\frac{\ln(2)f_{\max_w}}{f_0} - 1\right)2^{f_{\max_w}/f_0}\right). \quad (31)$$

The maximum throughput is calculated by inserting (30) into (29) and integrating over $[0, f_{\max_w}]$:

$$\frac{R_w}{f_0} = \frac{1}{f_0}\int_0^{f_{\max_w}} \log_2\left(\frac{|H(f)|^2}{|H(f_{\max})|^2}\right)df = \frac{1}{2}\left(\frac{f_{\max_w}}{f_0}\right)^2. \quad (32)$$

For a given γ, the optimum modulation bandwidth and the throughput are implicitly given by the inverse of (31) and by (32), respectively. Practical algorithms such as Hughes-Hartogs (HH) [21], [22] provide an iterative, discretized algorithm to calculate the optimum bit and power loading distribution. In [5], a good match between the theoretical throughput and the throughput achieved by discrete constellations using HH is shown. It optimizes the throughput, however, with high complexity and large overhead in communicating the used constellation on all sub-carriers.

C. OFDM WITH PRE-EMPHASIS

A simpler implementation is to pre-emphasize the channel and to use the same constellation for all sub-carriers. Pre-emphasizing implies a forced inversion of the channel response at the transmitter to compensate its low–pass behaviour. This is often referred to as a bandwidth extension, but comes at a penalty. Such pre-emphasis tends to defeat the advantage of OFDM to load every frequency bin optimally, thus is counterproductive. Nonetheless, we see IEEE 802.11bb standardization proposals to reuse WiFi-like OFDM schemes with constant constellations for OWC, to use existing IC designs. Our results will show that repairing the frequency response to support a fixed constellation can be reasonable in the lower NPB ranges, but the transmit bandwidth needs to be made adaptive to the NPB.

1) ARBITRARY MODULATION CONSTELLATIONS:

A filter inverts the LED low–pass response in the frequency range $[0, f_p]$. The throughput R_p is derived from (29) and (8) with the back-off κ given in (9):

$$\frac{R_p}{f_0} = \left(\frac{f_p}{f_0}\right)\log_2\left(1 + \frac{\gamma \ln 2}{\Gamma\left(2^{f_p/f_0} - 1\right)}\right). \quad (33)$$

The optimum modulation bandwidth, denoted by $f_{\max_p}$, to maximize the throughput is calculated from $dR_p/df_{\max_p} = 0$, which depends only on γ, f_0 and Γ [5].

2) DISCRETE MODULATION CONSTELLATIONS

Using discrete M, in (33), we cannot get tractable expressions for the derivatives w.r.t. spectral density. As an alternative optimization track, we exploit the fact that all sub-carriers carry the same constellation size M. In the previous subsection, we implicitly assumed a continuous-valued M, but in this section, we assume an M^2-QAM modulation that can only take integer values of an even power of 2 ($M = 2, 4, 8, ..$) and identical on all sub-carriers. We use the relation (23) to express ϵ_N/N_0 in terms of SNR(f), as in (6) but with a pre-emphasized spectral density (8),

$$\frac{2\epsilon_N(f)}{N_0} = \frac{\sigma_{mod}^2 H_0^2}{N_0 f_0}\frac{\ln 2}{2^{(f_p/f_0)} - 1}. \quad (34)$$

Our optimization tests various M and for each M value, the optimum modulation bandwidth f_p is taken such that ϵ_N/N_0 just exceeds $X(M)$. This results in

$$\frac{f_p}{f_0} = \log_2\left\{\frac{\gamma \ln(2)}{2X(M)} + 1\right\}, \quad (35)$$

1. Gross rate before coding.

which is identical to (22). The throughput for pre-emphasized OFDM employing M^2-QAM modulation scheme on all sub-carriers is calculated from

$$\frac{R_p}{f_0} = \frac{f_p}{f_0} \cdot \log_2 M^2, \tag{36}$$

which reduces to (16). In conclusion, for the same NPB γ, thus not yet considering the bias penalty on a pre-emphasized channel, both PAM and pre-emphasized OFDM schemes demand the same optimum modulation bandwidth and provide identical throughput and, therefore, the modulation bandwidth and throughput plots of Figure. 1 are also applicable for DCO-OFDM employing M^2-QAM.

Figure. 1 also includes the required modulation bandwidth and the throughput for pre-emphasized OFDM (blue lines) and for waterfilling (black lines) with continuous modulation order M at BER $= 10^{-4}$. As expected, waterfilling provides the maximum throughput. Pre-emphasis comes with a penalty in throughput, which increases with NPB but is small for low NPB. However, pre-emphasis requires less bandwidth. This can reduce the sampling rate, hence it consumes less power in analog-to-digital conversion and in digital signal processing. Furthermore, pre-emphasis avoids the need to exchange the bit loading profile, thus it reduces signalling overhead.

In Figure. 1(b), we see a small artefact due to simplifying Γ: OFDM with discrete M (red line) cannot outperform OFDM with continuous M (blue line). This artefact is small. Comparing the maximum normalized modulation bandwidth, continuous M does not show any jump in the optimized modulation bandwidth, which was also observed in [5].

Fixing the bandwidth means operating on a point on a horizontal line in Figure. 1(a). For operational points on this line, the link collapses if it is above the curves of the calculated maximum supportable $f_{\max}$. As an example, if a system with an LED of $f_0 = 10$ MHz fixes the transmit bandwidth to 40 MHz, it operates on the horizontal line of a normalized modulation bandwidth of 4. Below an NPB of about 25 dB, it uses a bandwidth broader than what PAM or pre-emphasized OFDM can support (the point of operation is above the plotted curves). Nonetheless, a well-performing link would be feasible if the system were allowed to scale back the bandwidth, rather than to aggressively push symbol rates beyond the 3 dB LED bandwidth.

V. CLIPPING AND DISTORTION MODEL

The modelling of clipping and distortion is subject to improving insights [31]. In the following we discuss three models

- Double sided clipping: In the early days, LEDs had to be designed for maximum power output. Above a certain current level, the LED would thermally break down. This justified a model in which the LED current is both non-negative and peak-limited [18].
- Clipping of the current: Today's LEDs are operated at a set point where the photon output per recombining electron-hole pair is the highest. This is far below any clipping point or breakdown rating. At higher currents, the LED efficiency only gradually reduces (LED droop). This justifies a single-sided (non-negative) clipping model [5], [11], [17], [31]. Similarly, many practical electronic drivers do not allow a negative current through the LED.
- Droop: Above their most efficient point, the LED becomes somewhat less efficient. This 'droop' leads to invertible second–order distortion, inherent to non-linear photon generation rates [38]–[40].

In this article we focus on the second model, but we also discuss the consequences of droop, as in the third model. In OFDM, the LED AC current, $i_{led}(t)$, has in good approximation a Gaussian probability density. It has rms modulation depth σ_{mod}. To ensure that the signal remains in the linear region, a DC bias I_{LED} is needed for the LED. Further, the LED imposes a low-pass nature, but studying memory effects in distortion is beyond the scope of this article.

A. CURRENT CLIPPING

The choice of z (defined in (17)) needs to ensure that the clipping noise stays below the maximum tolerable noise floor. From arguments in [5], [17], [31], we conclude that modern LEDs clip negative currents but are not peak limited in their operational range. The clipping noise per sample is zero if the signal $i_{led}(t) \geq -z\sigma_{mod}$ (or $I_{LED} \geq 0$) and equal to $i_{led} + z\sigma_{mod}$ otherwise. Using a Gaussian pdf for I_{LED} with mean value $z\sigma_{mod}$ and variance σ^2_{mod} and integrating over $\xi = i_{LED} - z\sigma_{mod}$, the i-th moment of the clipping is

$$\mu_i = \int_{-\infty}^{-z\sigma} \frac{(\xi + z\sigma_{mod})^i}{\sqrt{2\pi}\sigma_{mod}} \exp\left(-\frac{\xi^2}{2\sigma^2_{mod}}\right) d\xi. \tag{37}$$

The effective noise variance of the distortion is $\sigma_D^2 = \mu_2 - \mu_1^2$ and is calculated as

$$\frac{\sigma_D^2}{\sigma^2_{mod}} = \left(z^2+1\right)Q(z) - zg(z) - (g(z) - zQ(z))^2, \tag{38}$$

where $Q(.)$ and $g(.)$ are the tail distribution function and pdf of the standard normal distribution, respectively. For ease of notation, we introduce $c_z = \sigma_D/\sigma_{mod}$.

Clipping also attenuates the signal, particularly if $z < 2$. Below $z = 1$, where the signal level is multiplied by $a_z = 0.84$ [17], the effect becomes pronounced. While we refer the reader to [17] for expressions that relate z and a_z, we use a_z in following throughput equations.

We argue that the clipping spectrum is limited to f_x and does not significantly spill over to empty sub-carriers far above f_x: A signal spectrum limited to f_x, creates time–domain signals that are highly correlated in a period $f_x^{-1}/2$. Every clipping event causes an error signal that has a typical duration of about $f_x^{-1}/2$. By virtue of properties of Fourier Transforms and as we confirm by simulation, this leads to a clipping noise spectrum that is mainly restricted to $(0, f_x)$. Oversampling, and using an oversized FFT with broader

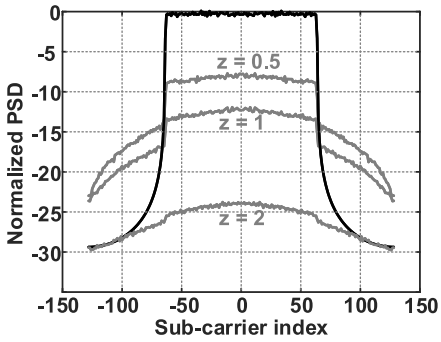

FIGURE 2. PSD of an OFDM signal (black) and clipping noise (gray), for bias ratio of 0.5, 1 and 2. LED low-pass response not included.

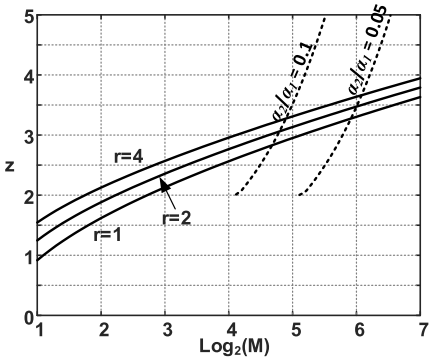

FIGURE 3. Bias ratio z versus number of bits $b = \log_2 M$ per sub-carrier in one dimension. Noise-free ($r = 1$) and leaving a 3 and 6 dB power margin ($r = 2$ and $r = 4$, respectively) to operate over a noisy channel. Solid line: clipping limit. Dashed line: invertible distortion limit. For distortion–limited z, we used $r = 1$.

bandwidth ($f_s \gg f_{max}$) sees clipping artefacts that span multiple time samples, but oversampling does not increase their bandwidth. Multiple independent clipping events add incoherently on a particular victim sub-carrier. Here, we refine the clipping noise model of [12], [17] that considers low-pass filtering of flat (spectrally white) clipping artefacts in the LED. Figure. 2 shows the PSD of 64-QAM ($M = 8$) on the 64 lower sub-carriers in an OFDM system with 128 sub-carriers thus with an IFFT size of 256. The PSD of the clipping noise is shown in Figure. 2 for $z = 0.5$ (overly aggressive clipping), $z = 1$ and $z = 2$. This plot confirms our argument that the clipping noise is mostly confined within the modulation bandwidth of the signal where it may have two or three dB variations. Also, the clipping PSD raises with lowering z. For the signal in Figure. 2, $z \geq 2.2$ is required to achieve a simulated BER of $< 10^{-4}$.

As clipping noise raises the noise floor, we model $N_0 \rightarrow N_0 + N_D(f)$. We approximate the simulated clipping spectra by a rectangular function within the modulation bandwidth f_x:

$$N_D(f) \approx \frac{\sigma_D^2}{f_x}|H(f)|^2 = \frac{c_z^2\sigma_{mod}^2|H(f)|^2}{f_x}. \tag{39}$$

B. INVERTIBLE DISTORTION MODEL

The hard clipping model of the LED needs refinement as other (invertible) non-linearities may dominate for high z. Electrons and holes recombine at a rate governed by the ABC formula [38]–[40]. For a brief discussion here, we simplify the dynamic model [30], [31], [39] by describing the light output ϕ as a function of LED current,

$$\phi = \alpha_1 I_{LED} + \alpha_2 I_{LED}^2 + \alpha_3 I_{LED}^3.$$

Modulating with $I_{LED} = \mathrm{I}_{LED} + i_{led}$, the signal ϕ sees second–order distortion with a relative strength

$$\begin{aligned}\frac{\sigma_{2D}^2}{\sigma_{mod}^2} &= \frac{(\alpha_2 + 3\alpha_3 \mathrm{I}_{LED})^2 \mathrm{E}\{i_{led}^4\}}{\left(\alpha_1 + 2\alpha_2 \mathrm{I}_{LED} + 3\alpha_3 \mathrm{I}^2_{LED}\right)^2 \mathrm{E}\{i_{led}^2\}} \\ &= \frac{3}{z^2}\frac{\left(\frac{\alpha_2}{\alpha_1} + \frac{3\alpha_3}{\alpha_1}\mathrm{I}_{LED}\right)^2 \mathrm{I}^2_{LED}}{\left(1 + \frac{2\alpha_2}{\alpha_1}\mathrm{I}_{LED} + \frac{3\alpha_3}{\alpha_1}\mathrm{I}^2_{LED}\right)^2}\end{aligned} \tag{40}$$

where σ_{2D}^2 is the variance of the second–order distortion and we used that, for a Gaussian distribution, $\mathrm{E}\{i_{led}^4\} = 3(\mathrm{E}\{i_{led}^2\})^2 = 3\sigma_{mod}^2$ and inserted $z^2 = \mathrm{I}_{LED}^2/\sigma_{mod}^2$. Based on our observations, the second–order distortion is the dominant distortion in LEDs for $z > 2$, hence we can neglect the term α_3 and the distortion caused by the third order non-linearity. The distortion i_{led}^2 is uncorrelated with the LED modulation current i_{led}, i.e., $\mathrm{E}\{i_{led}^2 \cdot i_{led}\} = 0$. Its spectrum, $N_{2D}(f)$ can be calculated by the convolution of the modulation spectrum of i_{led} by itself.

VI. EFFECT OF CLIPPING AND DISTORTION ON OFDM

In the following, we discuss two different approaches to handle the clipping noise.

A. CONSERVATIVELY CHOOSING LOW MODULATION DEPTH

A pragmatic (but not optimum) approach is to ensure the clipping noise spectrum falls below the receiver noise level. This can be translated into a requirement on the Signal-to-Distortion Ratio (SDR),

$$\mathrm{SDR} = \frac{2\epsilon_N}{N_D} = \frac{a_z^2}{c_z^2} \geq 2rX(M), \tag{41}$$

for all f, where r is a design (power) margin. This, with (38) gives the maximum modulation order M that can be used for a given z. Thus, for a target modulation order M (for M^2-QAM), it specifies the minimum required LED bias. Figure. 3 shows the minimum z as a function of number of bits per sub-carrier in one dimension for margins $r = 1$, 2 and 4. It can be seen that for a typical modulation order of 64-QAM ($M = 8$), $z \geq 2.15$ (compared to the simulated $z \geq 2.2$ in Section V) and $z \geq 2.4$ are needed for $r = 1$ and $r = 2$, respectively.

The optimum modulation bandwidth and the throughput follow from (35) and (36), if the distortion can be assumed to be negligible compared to receiver noise. This requires the modulation depth and constellation size to satisfy (41) for the given z with an adequate margin factor $r \geq 1$. However,

choosing the distortion power just below the noise level ($r = 1$) may not be adequate, as the distortion raises the noise level by 3 dB. Since the distortion also has a low–pass spectrum response, this affects mainly the lower sub-carriers. Nonetheless, to avoid that clipping affects the BER at any sub-carrier, a margin $r \geq 1$ is needed.

Considering a channel limited by second–order distortion, thus clipping– and noise–free channels, (41) can be written as

$$\text{SDR} = \frac{\sigma^2_{mod}}{\sigma^2_{2D}} \geq 2rX(M).$$

Dashed lines in Figure. 3 also show the minimum required z for margin $r = 1$ for two values of α_2/α_1 when $\text{I}_{\text{LED}} = 0.3$ A. It can be seen that for modulation order of $M \leq 16$, thus 256 QAM, the minimum z (for this specific example) is dominated by the clipping noise and the distortion is negligible. Values in the range of a Signal–to–Distortion–and–Noise Ratio (SNDR) around 40 dB are achieved in commercial ITU G.9991 systems, allowing up to 1024-QAM ($M = 32$), or 4096-QAM ($M = 64$) at maximum. The steep dashed curves confirm the practical experience that modulation orders above $M = 64$ are hard to achieve at reasonable z. In future systems, the distortion may be overcome by a pre or post-distortion compensation method, such as in [8]. Therefore, we do not elaborate on invertible distortion as limiting the throughput, so we focus on non-invertible clipping.

B. OPTIMIZING FOR THROUGHPUT

In this section, we include the clipping distortion power in our optimization of the modulation bandwidth and the throughput. Recalling (23), the received QAM symbol energy to noise plus distortion ratio (SNDR) is, using (39),

$$\text{SNDR}_{\text{OFDM}} = \frac{2\epsilon_N}{N_0 + N_D(f)} = \frac{a_z^2 S_x(f)|H(f)|^2}{N_0 + \frac{c_z^2 \sigma^2_{mod}}{f_x}|H(f)|^2}. \quad (42)$$

where x stands for pre-emphasis (p) or waterfilling (w).

1) THROUGHPUT OF PRE-EMPHASIS WITH DISTORTION

Inserting $S_p(f)$ and κ from (8) and (9), respectively,

$$\text{SNDR}_{\text{OFDM}} = \frac{\gamma \ln 2}{2^{f_p/f_0} - 1} \cdot \frac{a_z^2}{1 + \frac{c_z^2 \gamma 2^{-f/f_0}}{f_p/f_0}}. \quad (43)$$

For $z \to \infty$, $c_z \to 0$, $a_z \to 1$, and (43) reduces to (34) which was derived for clipping–free modulation. The above equations (42) and (43) are based on the effective energy emitted per symbol, thus do not reflect that with increasing z, more bias power is needed to achieve ϵ_N.

For a continuous modulation order M, one can replace the SNDR into (29) and solve the integral numerically for different f_p choices to optimize f_p for a given z. Pre-emphasis can achieve a normalized throughput of

$$\frac{R_p}{f_0} = \int_0^{f_p/f_0} \log_2\left(1 + \frac{1}{\Gamma}\frac{\gamma \ln 2}{2^{f_p/f_0} - 1} \cdot \frac{a_z^2}{1 + \frac{c_z^2 \gamma 2^{-x}}{f_p/f_0}}\right) dx. \quad (44)$$

The above integral has a closed form solution,

$$\begin{aligned}\frac{R_p}{f_0} = \frac{R_p(z \to \infty)}{f_0} + \frac{1}{(\ln 2)^2} \\ \times \left(Li_2\left(\frac{-c_{z_n}^2 \gamma}{f_p/f_0} 2^{-f_p/f_0}\right) - Li_2\left(\frac{-c_{z_n}^2 \gamma}{f_p/f_0}\right)\right) - \frac{1}{(\ln 2)^2} \\ \times \left(Li_2\left(\frac{-c_z^2 \gamma}{f_p/f_0} 2^{-f_p/f_0}\right) - Li_2\left(\frac{-c_z^2 \gamma}{f_p/f_0}\right)\right), \quad (45)\end{aligned}$$

where $R_p(z \to \infty)$ is the throughput for the case of no clipping noise, given in (33), $Li_2(.)$ is the Spence function defined as

$$Li_2(z) \triangleq \int_0^z \frac{\ln(1-u)}{-u} du, \quad (46)$$

and

$$c_{z_n} = \frac{c_z}{\sqrt{1 + \frac{a_z^2}{\Gamma}\frac{\gamma \ln 2}{2^{f_p/f_0} - 1}}}. \quad (47)$$

The optimum modulation bandwidth for pre-emphasis, $f_{\max_p}$, is normalized to f_0 to create versatile, generically applicable curves in Figure. 4(a) with blue lines for $z \to \infty$ (solid blue) and $z = 2.5$ (dashed blue). The corresponding normalized rates are shown in Figure. 4(b). Reducing z from ∞ (thus allowing unbounded biasing power) to 2.5 at a constant γ, increases the optimum modulation bandwidth to leverage the better SNDR at higher frequencies. Nevertheless, the throughput is experiencing a considerable penalty, which is about 25% for a γ of 50 dB. Increasing z from 2.5 to 3 reduces the penalty to about 10%.

More of practical use is a discrete constellation size M for M^2-QAM modulation. The calculated SNDR is an increasing function of frequency, that is, the minimum SNDR occurs at low frequencies. For the communication link to use the same constellation on all sub-carriers with the target BER, the choice of z needs to ensure that the required $X(M)$ can be satisfied at low frequencies,

$$\frac{\epsilon_N}{N_0 + N_D(0)} \geq X(M) \to \frac{\gamma \ln 2}{2^{f_p/f_0} - 1} \cdot \frac{a_z^2}{1 + \frac{c_z^2 \gamma}{f_p/f_0}} \geq 2X(M). \quad (48)$$

For a given γ and modulation order M, the optimum modulation bandwidth is the maximum f_p that satisfies (48). Unfortunately, a closed form expression for the optimum bandwidth cannot be derived. In the limiting case of clipping–free communication, our result reduces to (35). For a given γ and a given choice of z, the modulation bandwidth f_p is optimized from (48) as a function of M, so the throughput follows from (36). The optimum modulation order M is

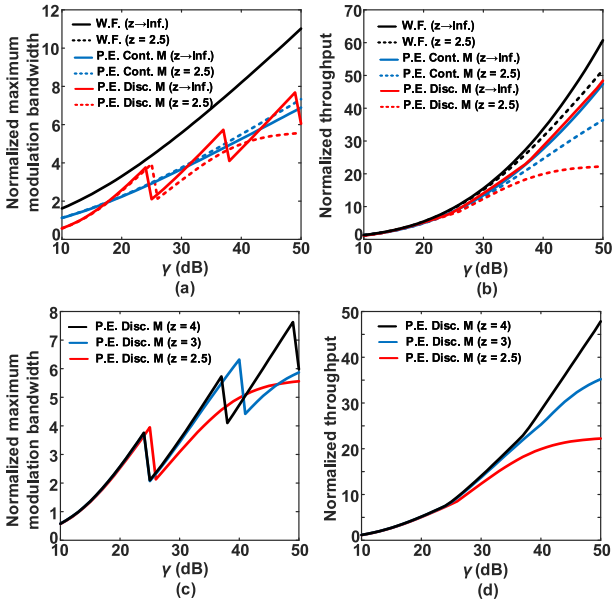

FIGURE 4. Normalized maximum modulation bandwidth and throughput for (a,b) waterfilling (W.F.), pre-emphasis (P.E.) with continuous (Cont.) and discrete (Disc.) modulation order M and (c,d) for pre-emphasis with discrete M, and different values of z as a function of γ. The BER is fixed at 10^{-4}.

the one that gives the highest throughput and the corresponding normalized modulation bandwidth is the optimum, $f_{\max_p}$. The throughput and $f_{\max_p}$ are shown in Figures. 4(a) and (b) with red lines for $z = 2.5$ (dashed-red) and $z \to \infty$ (solid red) and in Figures. 4(c) and (d) for different z values.

The difference between the continuous and discrete constellation size M was discussed in Section IV for distortion–free modulation ($z \to \infty$). Considering distortion with $z = 2.5$, as in Figure. 4(b), shows a considerable cut in throughput when using a discrete M, compared to a non-practical non-integer modulation order M. The throughput shows a reduction of about 40% at γ of 50 dB (see dashed red and dashed-blue lines).

We see a very substantial throughput penalty if one has to stick to discrete constellations M that are a power of 2, which is understood from the discussions that led to (48). In fact, while pre-emphasis equalizes the SNR (derived from (43) for $c_z = 0$), it does not generically equalize the SNDR, which, tends to be worse at lower frequencies.

To mitigate this gap while still using a common equal constellation M, the transmitter can adjust (lower) the power for the sub-carriers at higher frequencies with a better SNDR. This approach, however, requires an adaptive power loading algorithm which increases the complexity. Another approach to recover the throughput of discrete M modulation scheme (compared to the theoretical dashed-blue line of Figure. 4(b)) is to use a higher DC current. Figure. 4(d) shows that increasing z from 2.5 to 3 can recover a big fraction of the loss; the penalty of using discrete M compared to continuous M is about 20% and compared to $z \to \infty$ is about 30%.

Figures. 4(c) and (d) show that for a fixed z and large γ, thus when distortion dominates over the noise and over invertible distortion, the modulation bandwidth converges to a constant. Having $\gamma \to \infty$ in (48),

$$\frac{(\ln 2)a_z^2 f_p/f_0}{c_z^2(2^{f_p/f_0}-1)} \geq 2X(M), \tag{49}$$

shows that f_p/f_0 only depends on M, irrespective of the NPB γ. The throughput in (36), which only depends on M and the modulation bandwidth, is also approaching to a constant at large γ values.

2) WATERFILLING WITH DISTORTION

In [5], it is shown that the presence of clipping noise does not affect the modulation bandwidth $f_{\max_w}$ that optimizes the throughput. Hence the modulation bandwidth versus NPB (31) also holds when there is clipping noise provided that the signal power is corrected for the attenuation factor a_z^2. Based on equations in this article, we quantify the throughput penalty due to distortion as

$$\frac{R_w}{f_0} = \frac{R_w(z\to\infty)}{f_0} + \frac{f_{\max_w}}{f_0}\log_2\left(1+\frac{c_z^2\gamma}{f_{\max_w}/f_0}2^{-f_{\max_w}/f_0}\right) + \frac{1}{(\ln 2)^2}\left(Li_2\left(\frac{-c_z^2\gamma}{f_{\max_w}/f_0}2^{-f_{\max_w}/f_0}\right) - Li_2\left(\frac{-c_z^2\gamma}{f_{\max_w}/f_0}\right)\right). \tag{50}$$

The throughput and the associated optimum modulation bandwidth are shown in Figures. 4(a) and (b) as a function of the NPB γ. Waterfilling provides a better performance compared to pre-emphasis but uses a larger modulation bandwidth, for both clipping–free and clipped communication. Choosing $z = 2.5$ reduces the throughput of waterfilling approach by a gap that increases with γ and that is about 18% at γ of 50 dB compared to $z \to \infty$.

VII. COMPARISON OF DCO-PAM AND DCO-OFDM

We compare the two modulation schemes, DCO-PAM and DCO-OFDM, for different power constraints at the transmitter side. For various power constraints at the transmitter, we calculate the portion of the power that contributes to the throughput versus biasing power. We redefine the NPB parameter that allows for a fair comparison of the schemes, considering that a particular σ_{mod} leads to different consumed powers.

A. EXTRA–POWER LIMITED CHANNEL

For VLC links, the illumination power is available already ($\beta_1 = 0$) and only the extra power which is needed for modulation is of interest. Extra power was shown to be directly related to the LED current variance through the factor R_{LED}. The LED resistance R_{LED} consists of two parts, $R_{LED} = V_T/\mathrm{I}_{LED} + R_s$, where the dynamic part is an inverse function of I_{LED} and the second part is the constant parasitic resistance R_s. For LEDs biased at a typical current of $\mathrm{I}_{LED} =$ 0.35 A and with V_T being 25 mV, the dynamic resistance becomes approximately 70 mΩ which is negligible compared

to the R_s which is typically in the order of $1-2\ \Omega$ [33]. As a result, identical extra power for both modulation schemes is translated into identical σ_{mod}, hence the same NPB for both schemes. In Section IV and Figure. 1, it was shown that for the same NPB, thus ignoring biasing power and taking adequate z (no significant distortion), both schemes achieve the same throughput in a pre-emphasized channel. In fact, one may interpret the FFT with Hermitian symmetry, as used in OFDM, as just a unitary rotation of the PAM time signals along the time-frequency domains. OFDM preserves the number of dimensions and the distances in the signal space, thus in a pre-emphasized channel has equal spectrum efficiency and BER as PAM.

B. OPTICAL–POWER LIMITED CHANNEL

Optical power limitations can be induced for instance in VLC where illumination dictates the light level or in IR where eye-safety needs to be guaranteed. The average optical power of an LED can be written as [8]

$$P_{opt} = \frac{\langle E_p \rangle}{q} \mathrm{I}_{LED}, \tag{51}$$

where $\langle E_p \rangle$ is the average energy of the photons transmitted by the LED and q is the unit electron charge. According to (51), constraining the average optical power is equivalent to constraining the LED DC current via β_1 ($\beta_2 = 0, \beta_3 = 0$).

As we compare DCO-PAM and DCO-OFDM for the same LED DC current, their variances differ. The variance σ^2_{mod} is related to I_{LED} via z in (17). To reflect this, we use γ_{opt} as a variant of γ that addresses the optical power limit:

$$\gamma_{opt} = \frac{q^2 P^2_{opt}}{\langle E_p \rangle^2} \cdot \frac{H_0^2}{N_0 f_0}. \tag{52}$$

Then from (51), (52) and using the definition of z, the optical NPB relates to γ via

$$\gamma_{opt} = z^2 \gamma. \tag{53}$$

DCO-PAM has a lower PAPR, thus allows a smaller z than DCO-OFDM, hence gets a better γ for the same γ_{opt}. This implies a horizontal shift that differs per modulation setting. This changes the cross-over points for the choice of modulation that performs best for a given NPB. Using (17) for M-PAM with $M = 4, 8, 16$ and 32, $1/z^2$ is equivalent to horizontal shifts of 2.55, 3.68, 4.23, and 4.5 dB, respectively.

For OFDM, the bias ratio z is subject to optimization. We see in Figure. 5 that for pre-emphasized OFDM with a fixed z the throughput converges to a constant for large γ_{opt}, thus when clipping dominates over the noise floor. On the other hand for small γ_{opt}, when distortion is negligible, increasing z just leads to a reduction in the received SNR. Hence, at low γ_{opt}, the throughput curves of pre-emphasized DCO-OFDM are horizontally shifted copies of each other; the distance between the curves for $z = 2.5$ and $z = 4$ is significant: 4 dB.

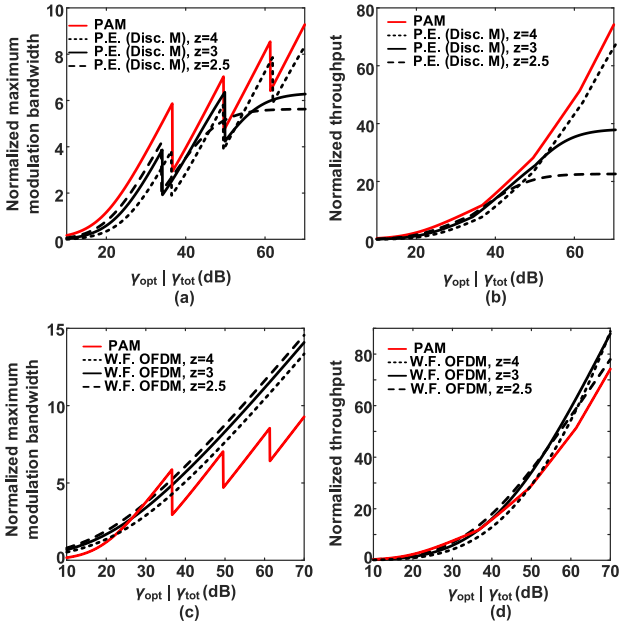

FIGURE 5. (a,c) Optimum (normalized) modulation bandwidth and (b,d) throughput versus optical NPB γ_{opt} for PAM (red lines) and OFDM (with pre-emphasis and with waterfilling) with different z choices. For all plots BER = 10^{-4}.

1) HIGH NORMALIZED POWER BUDGETS

As an example, for an LED with $f_0 = 10$ MHz bandwidth, to reach a throughput near a gigabit ($R_p/f_0 = 100$), $z = 4$ is needed, but that significantly jeopardizes the throughput for more distant receivers (with lower available NPBs) where $z < 3$ needs to guarantee range. In another example, to provide a throughput of $60f_0$, DCO-PAM requires an about 2.5 dB lower NPB compared to pre-emphasized DCO-OFDM while $z = 4$ is used for OFDM. Keeping the bias ratio of OFDM at $z = 4$, at a lower throughput of $10f_0$, the NPB difference between DCO-PAM and pre-emphasized DCO-OFDM increases to about 5 dB while a lower z, e.g., $z = 2.5$ shows only 1.6 dB NPB difference. We acknowledge that if pulse shaping of PAM is needed, the advantage shrinks, as z rises.

Interestingly, DCO-PAM also outperforms DCO-OFDM with waterfilling at low optical NPBs. Waterfilling performs better when the optical NPB increases, say γ_{opt} above 32 dB for $z = 2.5$ (equivalent to γ more than 24 dB) and above 50 dB for $z = 4$ (equivalent to a NPB γ of more than 38 dB[2]). The cross-over point for waterfilled DCO-OFDM to outperform PAM moves to higher NPBs when a higher z is selected. However, at large NPBs of 50 dB, the theoretically optimum modulation bandwidth for DCO-PAM is around $7f_0$. In practice, these large bandwidth extensions impose difficulties in the implementation.

2) LOW NORMALIZED POWER BUDGETS

At low NPBs, it may be attractive to use dedicated non-negative OFDM variants, such as ACO-OFDM or Flip

2. which is equivalent to a received electrical SNR of 23 dB in the modulation bandwidth of $f_{\max_w} \approx 7.5 f_0$ [5].

TABLE 3. Quick comparison of the linear and quadratic terms in the power consumption and a penalty on the SNR for flat channel (low NPB, small modulation bandwidth).

	Linear	Quadratic	SNR
PAM	$\sqrt{3\frac{M-1}{M+1}}\sigma_{mod}$	σ^2_{mod}	
DCO	$z\sigma_{mod}$	σ^2_{mod}	reduced by a_z^2 and $N_D(f)$
Flip/ACO	$\sqrt{2/\pi}\sigma_{mod}$	σ^2_{mod}	reduced by 50%

OFDM, to avoid the power losses in the DC bias. Flip OFDM carries the signal with variance σ^2_{mod}, however, samples with positive polarity are transmitted in a first block, negative samples are transmitted in flipped polarity in a second block. This ensures that a signal sample is always transmitted, thus it retains σ^2_{mod}, but the transmission time doubles. During reception, two blocked are folded back into one block to recover the full signal. It has been noticed [19], [41]–[43], that this operation collects noise from two blocks, thus reduces the SNR by one half. This, to a large extent, defeats the gain obtained from trying to avoid the DC-bias.

At high NPBs, these non-negative OFDM variants are outperformed by DCO-OFDM, also because at high SNR, a spectrum efficiency loss is incurred in Flip-OFDM by transmitting a second block: This demands higher constellations to squeeze more bits into fewer dimensions [19]. At low NPBs, where LED bandwidth is adequate to carry a low-rate signal, the lower mean value of Flip-OFDM appears beneficial [19]. The signal in the collapsed block has an effective symbol energy jointly equal to σ^2_{mod} but is processed over a single block time. The mean value of the signal is $\sqrt{2/\pi}\sigma_{mod} \approx 0.80\sigma_{mod}$. Table 3 lists the resulting linear and quadratic factors in the power consumption (3).

For optical–power limited channels, we take $\beta_2 = 0$. Flip OFDM[3] provides the maximum available σ_{mod} within a constrained β_1. Despite the 50% drop in the SNR of ACO/Flip OFDM, these appear to be slightly more attractive than PAM for large M: The FFT shapes the almost uniform 2D PAM signal probability density into a one-sided Gaussian, which appears to be beneficial. However, large modulation order are not suitable for weak links, which demand small M. For small and moderate M, straight PAM appears better than ACO-OFDM. From Figure. 3, we further see that DCO-OFDM performs comparably; by choosing a very low z. It severely clips, but 4-QAM ($M = 2$) DCO-OFDM is nonetheless feasible.

C. ELECTRICAL–POWER LIMITED CHANNEL

Often, the total electrical power (3) consumed is relevant. For a bias-T modulator, $\beta_1 = \mathrm{V}_0$ and $\beta_3 \approx R_s$ dominate (3), while $\beta_2\sigma^2_{mod}$ is much smaller. In fact, for a typical LED bias current of $\mathrm{I}_{LED} = 0.35$ A, $V_0 = 2.5$ V and $R_s = 1\ \Omega$, in the total electrical power equation (3), $\beta_1\mathrm{I}_{LED} = 0.875$, $\beta_2\sigma^2_{mod} = \beta_2\mathrm{I}^2_{LED}/z^2 = 0.1225/z^2$ and $\beta_3\mathrm{I}^2_{LED} = 0.1225$. For OFDM, typically $z > 2$, hence the term $\beta_2\sigma^2_{mod}$ is negligible.

3. Alternatively one many argue that clipping halves the ACO-OFDM power by 50%. So, to compare for the same signal power, we boost the ACO power by a factor of two, and also arrive at full σ^2_{mod}.

For PAM, however, z can be as low as 1 (for $M = 2$) and the approximation $\beta_2\sigma^2_{mod} \approx 0$ results in about 10% error (0.46 dB) in the total electrical power. The total electrical power can reasonably be approximated by the LED DC power consumption:

$$P_{tot} \approx \mathrm{V}_{\mathrm{LED}}\mathrm{I}_{LED} = \mathrm{V}_{\mathrm{LED}}z\sigma_{mod}. \tag{54}$$

To acknowledge that $z^2\sigma^2_{mod}$ rather than σ^2_{mod} itself is constrained, let us compare systems for the total NPB γ_{tot} including bias losses as

$$\gamma_{tot} = z^2\sigma^2_{mod} \cdot \frac{H_0^2}{N_0 f_0}. \tag{55}$$

This $\gamma_{tot} = z^2\gamma$ is identical to the definition of (52). In this case, the curves of Figure. 5 also apply to electrical-power limited channel if the x-axis is read as γ_{tot} axis. Alternatively, it can be shown that, the electrical power model by [17], taking $\beta_2 = \beta_3$ and $\beta_1 = 0$ would lead to $\gamma_{tot} = (z^2 + 1)\gamma$ which we do not consider in this work.

1) DESIGN CHOICE FOR z

At constant total power, lowering z boosts the signal σ^2_{mod}, thus enhances ϵ_N and γ, but it also increases distortion. For example, systems optimized for large coverage spread their optical power over a large area, thus often have to operate with relatively small γ_{tot}, say of about 30 dB. Then $z = 2.5$ is more attractive than $z = 4$. The latter can improve the throughput for short range or for systems with narrow beams by 65% (from $4.2f_0$ to $6.9f_0$) and 50% (from $R = 4.2f_0$ to $6.2f_0$) improvement for waterfilling and pre-emphasis, respectively. The point where higher z (e.g., $z = 4$ to avoid clipping) preforms better than boosting the signal strength (say, $z = 2.5$) is around a γ_{tot} of 46 dB for pre-emphasis and of 62 dB for waterfilling. For a high speed link (several hundreds of Mbit/sec or several Gbit/sec) with an LED with a typical 3 dB bandwidth of $f_0 \approx 10$ MHz, a large γ_{tot} (e.g., more than 70 dB) is needed. In this range, a large fraction of the electrical power is burnt in DC biasing to limit the distortion. From Figures. 5(b) and (d), we learn that a z above 4 will be required to achieve a transmission rate of more than $80f_0$. Moreover, mitigating second-order distortion also becomes critical (see Figure. 3).

2) A TYPICAL EXAMPLE

Consider an OWC system limited by total power, with the channel frequency response given in (4). At 1m distance, a gain-to-noise ratio of 70 dB in a 1 MHz sub-carrier bandwidth requires

$$\frac{H_0^2}{N_0 \times 10^6} = 10^7 \rightarrow N_0 \approx 10^{-19}\left(V^2/Hz\right).$$

A 450 nm LXML-PB02-0023 blue LED was measured. It has a 3-dB bandwidth around $f_0 \approx 10$ MHz at $\mathrm{I}_{LED} = 350$ mA bias current [5] with $V_0 \approx 2.5$ V. Since the dominant term in

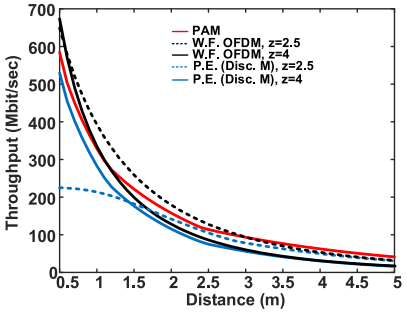

FIGURE 6. Throughput versus distance for PAM (red), pre-emphasized OFDM with $z = 2.5$ (dashed-blue) and $z = 4$ (solid-blue) and waterfilling with $z = 2.5$ (dashed-black) and $z = 4$ (solid-black). The total electrical power is limited to 1 W.

the total power consumption equation (3) is the DC power, from (1) we have

$$V_{LED} = 2.5V + (1\Omega) \times (0.35A) = 2.85V,$$

and

$$P_{tot} \approx P_{DC} = (2.85V) \times (0.35A) \approx 1W.$$

The total NPB is calculated from (54) and (55) to be 1.6×10^5, thus approximately 52 dB. For the 52 dB of γ_{tot}, the throughput can be found in Figures. 5(b) and (d) for DCO-PAM and DCO-OFDM using waterfilling or pre-emphasis strategies. Figure. 6 shows the throughput versus the distance between the transmitter and the receiver for different z values. To include the impact of distance d, we used the 4th power law ("40 log d") path loss model of [44]. With $\gamma_{tot,dB} = 10\log_{10}(\gamma_{tot})$,

$$\gamma_{tot,dB}(d) = 52 - 40\log_{10}\left(\frac{d}{1\text{m}}\right)$$

to ensure that at 1 m distance, γ_{tot} is 52 dB. Several relevant observations can be made. Waterfilling marginally outperforms DCO-PAM at distances below 1 m, while operating beyond 3 m, DCO-PAM provides the better performance. At a close distance (below 1 m for waterfilling and below 1.5 m for pre-emphasis), the received signal is sufficiently strong to focus merely on distortion. Therefore, a large z (e.g., $z = 4$ rather than a small $z = 2.5$) is required to provide the optimum performance. On the other hand, when the distance increases, the receiver noise floor becomes the dominant design concern and the transmitter has to boost the modulation depth, thereby compromising z and tolerating more clipping.

VIII. COMPUTATIONAL COMPLEXITY

Another important aspect for the comparison is the computational complexity of modulation at the transmitter and detection in the receiver. The complexity in the OFDM transmit Inverse Fast Fourier Transform (IFFT) and in the receive (FFT) of size N is in the order of $4N\log_2 N$ per block. For PAM, the use of simple pre-emphasis eliminates the need for equalization if only the low-pass LED response needs to be compensated. One can repair ISI at the receiver more effectively by using a DFE equalizer [16]. The latter can simultaneously handle channel multipath, if it occurs, and avoids too large noise enhancements, but at the cost of a complex Viterbi algorithm. Also frequency–domain, equalizers have been proposed, that place both an FFT and IFFT at the receiver. However, one may argue that the complexity of FFTs typically is small compared to other signal processing, such that the use of an FFT is not prohibitive. Possibly, the complexity of the signalling protocol, its over-head, and the number of memory operations in an OFDM system can be of concern. In this respect, waterfilling or uniform power loading may be less attractive as it places a different modulation order per sub-carrier, which needs to be negotiated between receiver and transmitter.

IX. CONCLUSION

The two popular OWC modulation schemes, namely Orthogonal Frequency Division Multiplexing (OFDM) and Pulse Amplitude Modulation (PAM) were compared for use in an IM/DD system using LEDs, considering the minimally required DC biasing to ensure the non-negativity of driving LED current. To cope with the LED channel response, two well-known OFDM power loading strategies were discussed, namely, waterfilling and the correction of the attenuation of higher frequencies by a pre-emphasis.

We derived mathematical expressions for the throughput and the optimum modulation bandwidth to be used. Using a suitable Normalized Power Budget (NPB) definition and a normalization to the LED 3 dB bandwidth, generic results could be derived. It was shown that for the same extra modulation power, which is a suitable metric for VLC where the DC bias is already available for illumination, pre-emphasized OFDM and PAM at a reduced modulation depth showed no difference in throughput and in required modulation bandwidth. Waterfilling, which is the optimum power allocation strategy, outperforms pre-emphasized systems, but occupies a larger required bandwidth.

The conclusions and optimally recommended choices, however, differ for channels that are limited by their optical power or by their electrical power. Optical power can be confined by limits to the illumination level in VLC or by eye safety precautions in IR. In IR communication, particularly with battery–powered devices, the total available electrical power may be limited. Here, the DC bias can be minimized, just to carry the data signal in an undistorted manner. OFDM suffers from a large peak-to-average ratio. The non-negativity constraint forces the use of an unattractively large bias. Compromising for a practical bias current for OFDM, peaks in the current have to be clipped before being applied to the LED. We quantified and modeled the resulting distortion and its impact on performance, which allows for an optimization of the modulation depth depending on, for instance, NPB. In this article, we generalized derivations for OFDM, both for waterfilling and for

pre-emphasis, by including the clipping noise in the throughput and bandwidth optimization. We showed that for an IR channel, more precisely, for optical–power limited channels, under moderate modulation bandwidth, M-PAM with a linear high-boost filter is able to provide a higher data transmission rate than any sub-carrier loading scheme, optimized for DCO-OFDM. When a large NPB is available, OFDM preferably with bit loading that follows waterfilling principles outperforms M-PAM.

The best LED bias setting depends on the NPB. Moreover, the cross point for the NPB at which waterfilling DCO-OFDM starts to outperform PAM moves towards higher NPB values when a higher bias current of the LED is selected. Therefore, an OFDM system with a fixed LED bias current which is designed to operate for a range of NPBs might underperform compared to PAM, if OFDM is optimized for low NPB range or for large coverage. Preferably, an adaptive setting of the LED bias current, optimized for the NPB is used to yield the highest DCO-OFDM throughput.

REFERENCES

[1] "Visible light communication (VLC)—A potential solution to the global wireless spectrum shortage," GBI Research, London, U.K., Rep. GBISC017MR, 2011. [Online]. Available: http://www.gbiresearch.com/

[2] H. Elgala, R. Mesleh, and H. Haas, "Indoor optical wireless communication: Potential and state-of-the-art," *IEEE Commun. Mag.*, vol. 49, no. 9, pp. 56–62, Sep. 2011.

[3] A. Jovicic, J. Li, and T. Richardson, "Visible light communication: Opportunities, challenges and the path to market," *IEEE Commun. Mag.*, vol. 51, no. 12, pp. 26–32, Dec. 2013.

[4] L. Grobe *et al.*, "High-speed visible light communication systems," *IEEE Commun. Mag.*, vol. 51, no. 12, pp. 60–66, Dec. 2013.

[5] S. Mardanikorani, X. Deng, and J.-P. M. G. Linnartz, "Sub-carrier loading strategies for DCO-OFDM LED communication," *IEEE Trans. Commun.*, vol. 68, no. 2, pp. 1101–1117, Feb. 2020.

[6] D. Tsonev, S. Sinanovic, and H. Haas, "Complete modeling of nonlinear distortion in OFDM-based optical wireless communication," *J. Lightwave Tech.*, vol. 31, no. 18, pp. 3064–3076, Sep. 2013.

[7] K. Ying, Z. Yu, R. J. Baxley, H. Qian, G.-K. Chang, and G. T. Zhou, "Nonlinear distortion mitigation in visible light communications," *IEEE Wireless Commun.*, vol. 22, no. 2, pp. 36–45, Apr. 2015.

[8] X. Deng *et al.*, "Mitigating LED nonlinearity to enhance visible light communications," *IEEE Trans. Commun.*, vol. 66, no. 11, pp. 5593–5607, Nov. 2018.

[9] J. Armstrong, "OFDM for Optical Communications," *J. Lightw. Technol.*, vol. 27, no. 3, pp. 189–204, Feb. 2009.

[10] S. C. J. Lee, "Discrete multitone modulation for short-range optical communications," Ph.D. dissertation, Dept. Electr. Eng., Technische Universiteit Eindhoven, Eindhoven, The Netherlands, 2009.

[11] D. J. F. Barros, S. K. Wilson, and J. M. Kahn, "Comparison of orthogonal frequency-division multiplexing and pulse-amplitude modulation in indoor optical wireless links," *IEEE Trans. Commun.*, vol. 60, no. 1, pp. 153–163, Jan. 2012.

[12] J. Lian, M. Noshad, and M. Brandt-Pearce, "Comparison of optical OFDM and M-PAM for LED-based communication systems," *IEEE Commun. Lett.*, vol. 23, no. 3, pp. 430–433, Mar. 2019.

[13] S. Dimitrov, S. Sinanovic, and H. Haas, "Signal shaping and modulation for optical wireless communication," *J. Lightw. Technol.*, vol. 30, no. 9, pp. 1319–1328, May 2012.

[14] *Photobiological Safety of Lamps and Lamp Systems*, British Standards BS EN 62471, Sep. 2008.

[15] A. Nuwanpriya, S.-W. Ho, J. A. Zhang, A. J. Grant, and L. Luo, "PAM-SCFDE for optical wireless communications," *J. Lightw. Technol.*, vol. 33, no. 14, pp. 2938–2949, Jul. 2015.

[16] D. J. F. Barros and J. M. Kahn, "Comparison of orthogonal frequency-division multiplexing and on-off keying in amplified direct-detection single-mode fiber systems," *J. Lightw. Technol.*, vol. 28, no. 12, pp. 1811–1820, Jun. 2010.

[17] X. Ling, J. Wang, X. Liang, Z. Ding, and C. Zhao, "Offset and power optimization for DCO-OFDM in visible light communication systems," *IEEE Trans. Signal Process.*, vol. 64, no. 2, pp. 349–363, Jan. 2016.

[18] S. Dimitrov and H. Haas, "Information rate of OFDM-based optical wireless communication systems with nonlinear distortion," *J. Lightw. Technol.*, vol. 31, no. 6, pp. 918–929, Mar. 2013.

[19] X. Deng, S. Mardanikorani, G. Zhou, and J.-P. M. G. Linnartz, "DC-bias for optical OFDM in visible light communications," *IEEE Access*, vol. 7, pp. 98319–98330, 2019.

[20] R. G. Gallager, *Information Theory and Reliable Communication*. New York, NY, USA: Wiley, 1968.

[21] D. Hughes-Hartogs, "Ensemble modem structure for imperfect transmission media," U.S. Patent 4 679 227, Jul. 1987.

[22] D. Hughes-Hartogs, "The capacity of a degraded spectral Gaussian broadcast channel," Ph.D. dissertation, Inf. Syst. Lab., Center Syst. Res., Stanford Univ., Stanford, CA, USA, Jul. 1995.

[23] J. A. C. Bingham, "Multicarrier modulation for data transmission: An idea whose time has come," *IEEE Commun. Mag.*, vol. 28, no. 5, pp. 5–14, May 1990.

[24] B. Cardiff, M. F. Flanagan, F. Smyth, L. P. Barry, and A. D. Fagan, "On Bit and Power Loading for OFDM Over SI-POF," *J. Lightw. Technol.*, vol. 29, no. 10, pp. 1547–1554, May, 2011.

[25] L. Goldfeld, V. Lyandres, and D. Wulich, "Minimum BER power loading for OFDM in fading channel," *IEEE Trans. Commun.*, vol. 50, no. 11, pp. 1729–1733, Nov. 2002

[26] "G.vlc: Draft," Int. Telecommun. Union, Geneva, Switzerland, Recommendation ITU-T G.9991, Sep. 2018. [Online]. Available: https://www.itu.int/md/T17-SG15-181008-TD-PLEN-0291

[27] *Status of IEEE 802.11 Light Communication TG*. Accessed: Jul. 2020. [Online]. Available: http://www.ieee802.org/11/Reports/tgbb-update.htm

[28] H. L. Minh *et al.*, "100-Mb/s NRZ visible light communications using a postequalized white LED," *IEEE Photon. Technol. Lett.*, vol. 21, no. 15, pp. 1063–1065, Aug. 2009.

[29] C. Chen, D. A. Basnayaka, and H. Haas, "Downlink performance of optical attocell networks," *J. Lightw. Technol.*, vol. 34, no. 1, pp. 137–156, Jan. 2016.

[30] S. Mardani, A. Alexeev, and J.-P. Linnartz, "Modeling and compensating dynamic nonlinearities in LED photon-emission rates to enhance OWC," in *Proc. SPIE Light-Emitting Devices Materials Appl.*, vol. 10940. San Francisco, CA, USA, Mar. 2019. [Online]. Available: https://doi.org/10.1117/12.2511099

[31] J. P. Linnartz, X. Deng, A. Alexeev, and S. Mardani, "Wireless communication over an LED channel," *IEEE Commun. Mag.*, to be published, 2020.

[32] X. Deng, K. Arulandu, Y. Wu, S. Mardanikorani, G. Zhou, and J.-P. M. G. Linnartz, "Modeling and analysis of transmitter performance in visible light communications," *IEEE Trans. Veh. Technol.*, vol. 68, no. 3, pp. 2316–2331, Mar. 2019.

[33] "Advance electrical design LED model," Lumileds, San Jose, CA, USA, Rep. AB20-3A, 2002.

[34] K. Arulandu, J.-P. M. G. Linnartz, and X. Deng, "Enhanced visible light communication modulator with dual feedback control," *IEEE Trans. Emerg. Sel. Topics Power Electron.*, early access, Dec. 30, 2019, doi: 10.1109/JESTPE.2019.2962999.

[35] S. Yoo, D. Yun, B. Song, J. Burm, J. Chung, and J. H. Chun, "A 10 Gb/s 4-PAM transceiver with adaptive pre-emphasis," in *Proc. ISIC*, Singapore, 2011, pp. 258–261.

[36] X. Huang, J. Shi, J. Li, Y. Wang, and N. Chi, "A Gb/s VLC transmission using hardware preequalization circuit," *IEEE Photon. Technol. Lett.*, vol. 27, no. 18, pp. 1915–1918, Sep. 2015.

[37] S. Haykin, *Communication Systems*, 3rd ed. New York, NY, USA: Wiley, 1994.

[38] J. Piprek, "Efficiency droop in nitride-based light-emitting diodes," *Phys. Status Solidi A*, vol. 207, no. 10, pp. 2217–2225, Oct. 2010.

[39] Q. Dai *et al.*, "On the symmetry of efficiency-versus-carrier concentration curves in GaInN/GaN light-emitting diodes and relation to droop-causing mechanisms," *Appl. Phys. Lett.*, vol. 98, no. 3, 2011, Art. no. 033506.
[40] H. Zhao, G. Liu, J. Zhang, R. A. Arif, and N. Tansu, "Analysis of internal quantum efficiency and current injection efficiency in III-nitride light-emitting diodes," *J. Display Technol.*, vol. 9, no. 4, pp. 212–225, Apr. 2013
[41] N. Fernando, Y. Hong, and E. Viterbo, "Flip-OFDM for optical wireless communications," in *Proc. IEEE Trans. Inf. Theory Workshop*, Paraty, Brazil, 2011, pp. 5–9.
[42] N. Fernando, Y. Hong, and E. Viterbo, "Flip-OFDM for unipolar communication systems," *IEEE Trans. Commun.*, vol. 60, no. 12, pp. 3726–3733, Dec. 2012.
[43] Z. Yu, R. J. Baxley, and G. T. Zhou, "Achievable data rate analysis of clipped FLIP-OFDM in optical wireless communication," in *Proc. IEEE Globecom Workshops*, Anaheim, CA, USA, 2012, pp. 1203–1207.
[44] A. Tsiatmas, C. P. M. J. Baggen, F. M. J. Willems, J.-P. M. G. Linnartz, and J. W. M. Bergmans, "An illumination perspective on visible light communications," *IEEE Commun. Mag.*, vol. 52, no. 7, pp. 64–71, Jul. 2014.

SHOKOUFEH MARDANIKORANI (Student Member, IEEE) received the B.Sc. degree in electrical engineering from the University of Shahrekord, Shahrekord, Iran, in 2012, and the M.Sc. degree in communication systems engineering from the Sharif University of Technology, Tehran, in 2014. She is currently pursuing the Ph.D. degree in electrical engineering with the Signal Processing Systems Group, Eindhoven University of Technology, Eindhoven, The Netherlands. Her main research interests include the application of information theory, system modeling and signal processing in optical wireless, and visible light communications.

XIONG DENG (Member, IEEE) received the M.Eng. degree in communication and information engineering from the University of Electronic Science and Technology of China, in 2013, and the Ph.D. degree in optical wireless communications from the Eindhoven University of Technology, Eindhoven, The Netherlands, in 2018. In 2013, he was a Researcher with the Terahertz Science and Technology Research Center, China Academy of Engineering Physics, where he was involved in the integrated terahertz communication and imaging system. He was a Guest Researcher with Signify (Philips Lighting) Research, where he was involved in light fidelity. He is currently a Postdoctoral Researcher with the Eindhoven University of Technology. His research interests include the system modeling, digital signal processing, circuits for intelligent lighting, millimeter wave, radio over fiber, and optical wireless communications. He serves as a Reviewer for multiple IEEE/OSA journals, including IEEE TRANSACTIONS ON INDUSTRIAL ELECTRONICS, IEEE JOURNAL OF EMERGING AND SELECTED TOPICS IN POWER ELECTRONICS, IEEE TRANSACTIONS ON COMPUTERS, IEEE TRANSACTIONS ON VEHICULAR TECHNOLOGY, IEEE JOURNAL OF LIGHTWAVE TECHNOLOGY, IEEE TRANSACTIONS ON COGNITIVE COMMUNICATIONS AND NETWORKING, IEEE COMMUNICATIONS LETTERS, IEEE PHOTONICS JOURNAL.

JEAN-PAUL M. G. LINNARTZ (Fellow, IEEE) received the M.Sc. degree (*cum laude*) from the Eindhoven University of Technology (TU/e), Eindhoven, The Netherlands, in 1986, and the Ph.D. degree (*cum laude*) from the Delft University of Technology (TU Delft), The Netherlands, in 1991. He was a Senior Director with the Philips Research, Eindhoven, where he headed Security, Connectivity, and IC Design Research Groups. He initiated research on Coded Light, to allow the embedding of identifiers in light sources, which is now being used in many office and retail facilities. He is currently a part-time Professor with the TU/e, addressing intelligent lighting systems and optical wireless communication, and a Research Fellow with Signify (Philips Lighting) Research. His inventions led to over 75 granted patent families and have been a basis for three ventures. His papers have been cited more than 11 000 times and his H-index is 53 (GS). From 1992 to 1995, he was an Assistant Professor with the University of California at Berkeley. In 1994, he was an Associate Professor with TU Delft. From 1988 to 1991, he was an Assistant Professor with the TU Delft. He is a Fellow of the IEEE for his leadership in Security with Noisy Data.